Nuclear Engineering and Design 381 (2021) 111338

Contents lists available at ScienceDirect

Nuclear Engineering and Design

journal homepage: www.elsevier.com/locate/nucengdes

# Neutron importance based lattice-to-core projection technique and its application for HTGR design using Monte Carlo method

Donny Hartanto [a,b], Peng Hong Liem [c,d,*]

[a] Department of Mechanical and Nuclear Engineering, University of Sharjah, P.O. BOX 27272, Sharjah, United Arab Emirates
[b] Nuclear Energy System Simulation and Safety Research Group, Research Institute for Sciences and Engineering, University of Sharjah, P.O. BOX 27272, Sharjah, United Arab Emirates
[c] Cooperative Major in Nuclear Energy, Graduate School of Engineering, Tokyo City University (TCU), 1-28-1 Tamazutsumi, Setagaya, Tokyo, Japan
[d] Scientific Computational Division, Nippon Advanced Information Service (NAIS Co., Inc.), 416 Muramatsu, Tokaimura, Ibaraki, Japan

ARTICLE INFO

*Keywords:*
HTTR
Optimum fuel
Neutron importance
Serpent
ENDF/B-VIII.0

ABSTRACT

In general, a nuclear core design process is divided into two subsequent phases, namely the fuel lattice design phase, and followed by the full core design phase such as for the light water reactor (LWR). The optimal design parameters obtained from the fuel design phase can be used in a straightforward manner in the full core design phase since the neutron mean free path is much smaller than the fuel assembly dimensions. Unfortunately, the above-mentioned favorable situation may not be applicable for a high-temperature gas-cooled reactor (HTGR) design process. In this paper, for the HTGR design process, we propose a new technique based on the neutron importance concept to make a projection of the optimal design parameters obtained from the fuel design phase to the full core design phase so that the optimization works required in the full core design phase can be significantly reduced. The proposed technique is implemented in the Japanese High-Temperature Engineering Test Reactor to find the optimal fuel composition that can achieve an average core discharge burnup of 80 GWd/tU using single-batch and multi-batch refueling schemes. Important core neutronics parameters, such as reactivity coefficient and power profiles, are also discussed. Moreover, the impact of the axial shuffling scheme on the fuel compact fuel temperature is also analyzed.

## 1. Introduction

In the long and iterative process of nuclear core design which demands substantial computational resources, a technique capable of reducing the overall computation time is essential, especially when the continuous Monte Carlo method is adopted. In general, a nuclear core design process is divided into two subsequent phases, namely the fuel lattice design phase, and followed by the full core design phase. In the fuel lattice (or fuel assembly) design phase, numerous dominant design parameters and constraints covering the fuel composition, dimension, moderation ratio, target burnup, etc. are considered, however, the calculation geometry and domain are usually simple and small, and mostly in 2-dimensional (2-D). The main objective of the fuel lattice design is to find narrow ranges of optimal design parameters which can be used in the subsequent full core design phase. In the full core design phase, the free design parameters are usually fewer, but the calculation geometry may require a 3-dimensional (3-D) one with large spatial dimensions. In addition, when the burnup analysis is also conducted (which is the usual case) in the full core design phase, the core spatial domain has to be divided into many small burnup regions to guarantee the accuracy of the analysis results.

For a light water reactor (LWR), the optimal design parameters obtained from the fuel design phase can be used in a straightforward manner in the full core design phase since the neutron mean free path is much smaller than the fuel assembly dimensions. Another design aspect that supports this argument is the fact that an LWR core consists of only fuel assemblies. Only in the most outer regions (both radial and axial) of the core, an LWR designer places highly moderated reflectors to reduce neutron leakage. This implies that the neutron spectra in the core are not significantly different, although they may be slightly different from one type of fuel assembly to other types. The above-mentioned LWR design process is well represented by, for example, the use of CASMO5 (Rhodes

* Corresponding author at: Cooperative Major in Nuclear Energy, Graduate School of Engineering, Tokyo City University (TCU), 1-28-1 Tamazutsumi, Setagaya, Tokyo, Japan.
*E-mail address:* liemph@nais.ne.jp (P.H. Liem).

https://doi.org/10.1016/j.nucengdes.2021.111338
Received 27 April 2021; Received in revised form 7 June 2021; Accepted 16 June 2021

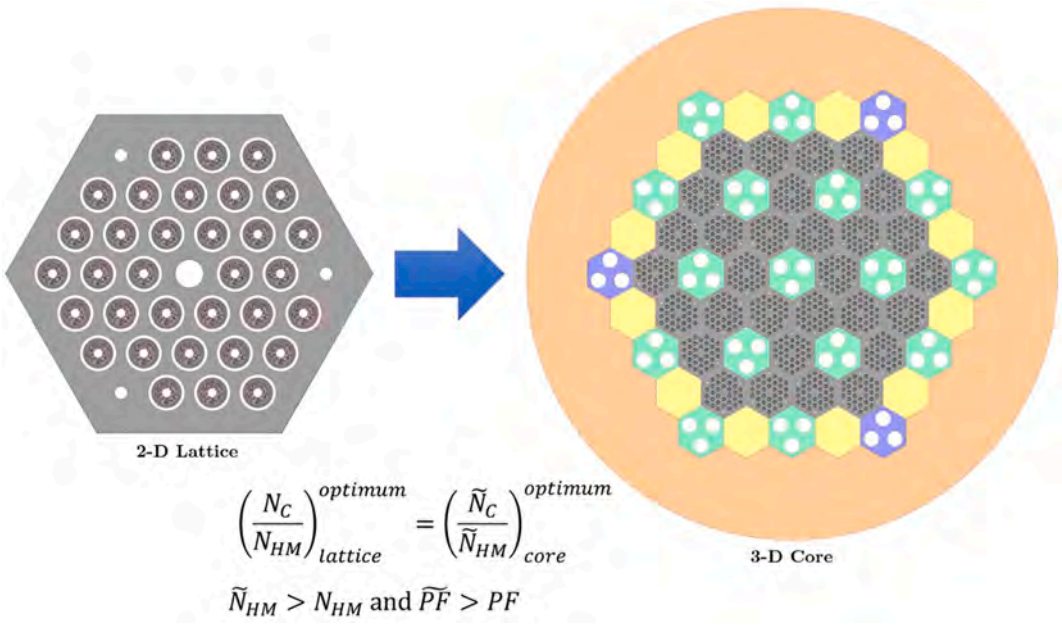


**Fig. 1.** Projection of optimum fuel lattice composition from lattice to core.

**Table 1**
Japanese 30 MWth HTTR Main Design Parameters.

| Power (MWth) | 30 |
|---|---|
| Coolant inlet/outlet temperature (°C) | 395/950 |
| Primary coolant pressure (MPa) | 4 |
| Equivalent core diameter (m) | 2.3 |
| Equivalent core height (m) | 2.9 |
| Average power density (W/cm$^3$) | 2.5 |
| Fuel | $UO_2$ |
| Enrichment (wt.%) | 3 to 10 |
| Burnup period (EFPD) | 660 |
| Fuel block | C |
| Coolant | He |
| Reflector thickness | |
| Top (m) | 1.16 |
| Side (m) | 0.99 |
| Bottom (m) | 1.16 |
| Number of fuel assemblies | 150 |
| Number of fuel columns | 30 |
| Number of pairs of control rods | |
| In Core | 7 |
| In Reflector | 9 |
| Number of instrumentation columns | 3 |

et al., 2006) and SIMULATE5 (Bahadir and Lindahl, 2009) codes during the fuel lattice design phase and full core design phase, respectively.

Unfortunately, the above-mentioned favorable situation may not be applicable for a high-temperature gas-cooled reactor (HTGR) design process for the following reasons. First, an HTGR commonly uses a graphite moderator, hence, the neutron mean free path is much longer than the fuel lattice dimensions. As an important consequence, the neutron spectrum in one region is affected by other regions which may not or cannot be considered during the fuel lattice design phase. Second, an HTGR core consists of not only fuel elements but also a large volume of graphite blocks (for prismatic/block-type HTGR) or graphite (dummy) pebbles (for a pebble-bed-type HTGR). Third, for safety purposes, the graphite reflectors are used not only in the outer regions of the core but also in the center of the core, namely the so-called annular core. For this particular configuration, the core thickness becomes thinner and the effect of inner and outer graphite reflectors becomes stronger.

Recently, continuous energy Monte Carlo codes, such as MCNP-6.2 (Werner, 2017), MVP-3 (Nagaya et al., 2017), Serpent 2 (Leppänen et al., 2015), etc. have been widely used in the design and analysis of nuclear reactors including HTGRs. These high-fidelity codes have features that are strongly demanded by the nature of the HTGR fuel and core, i.e. the capability to treat accurately the double-heterogeneity effect of TRISO (TRI-structural Isotropic) fuel particles (Price, 2012), pebble or pin fuel elements. The downside of Monte Carlo code utilization is the resource demanded and the long computation time, especially if it is used in the full core design phase with burnup analysis. This motivated us to develop a new technique that may reduce the number of full core Monte Carlo calculations to obtain an optimal fuel composition.

Previously a heuristic approach was used to project the core fuel compositions based on the optimal lattice fuel compositions using an approximation to get the "effective" $N_C/N_{HM}$ (carbon-to-heavy metal density ratio) between the lattice and the core (Hartanto and Liem, 2020). In this paper, for the HTGR design process, we propose a new technique based on the neutron importance concept to make a projection of the optimal design parameters obtained from the fuel lattice design phase to the full core design phase so that the optimization works required in the full core design phase can be significantly reduced. The essence of the proposed technique is to conserve the optimal neutronics condition, in terms of graphite to fuel nuclide density ratio, in both the fuel lattice design phase and the full core design phase.

The rationale of the proposed technique is given in Chapter 2. In Chapter 3, we will show the effectiveness of the proposed technique in designing small HTGRs. Chapter 4 summarizes our present work and discusses possible future work.

## 2. Rationale of the newly proposed technique

The newly proposed technique is performed in two steps. In the first step, the fuel composition of the fuel lattice is optimized to have a minimum fissile content per energy generated (kg/GWd). Extensive fuel block lattice burnup calculations with leakage-free boundary conditions are performed using continuous energy Monte Carlo code Serpent 2 and the latest nuclear data library ENDF/B-VIII.0 (Brown et al., 2018) by varying two design parameters which are the fissile content (% U-235) and the heavy metal (HM) loading per fuel block (kg HM). The HM loading per fuel block is equivalent to the TRISO particle fuel packing fraction (PF) and it influences the neutron spectrum and the neutron multiplication factor $k$. Meanwhile, the fissile content dictates the

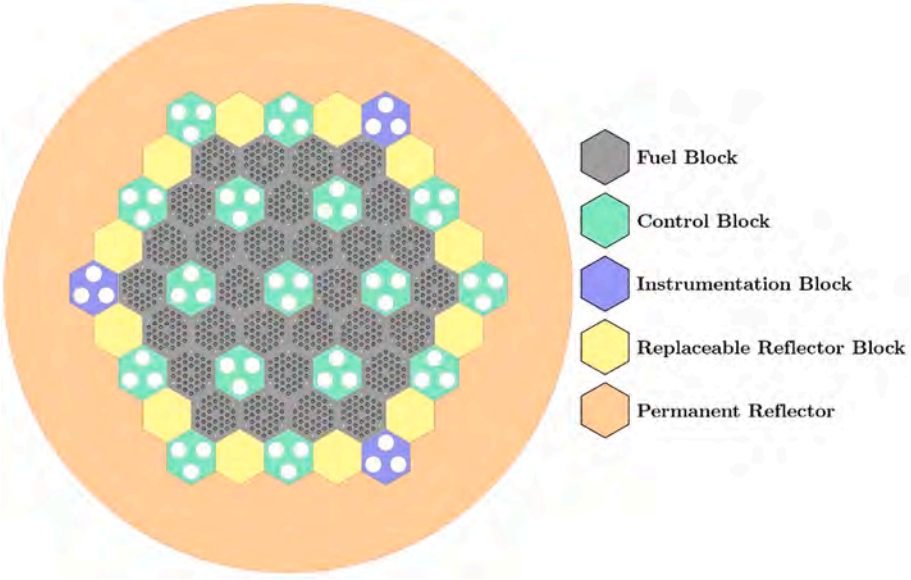


**Fig. 2.** The radial layout of HTTR.

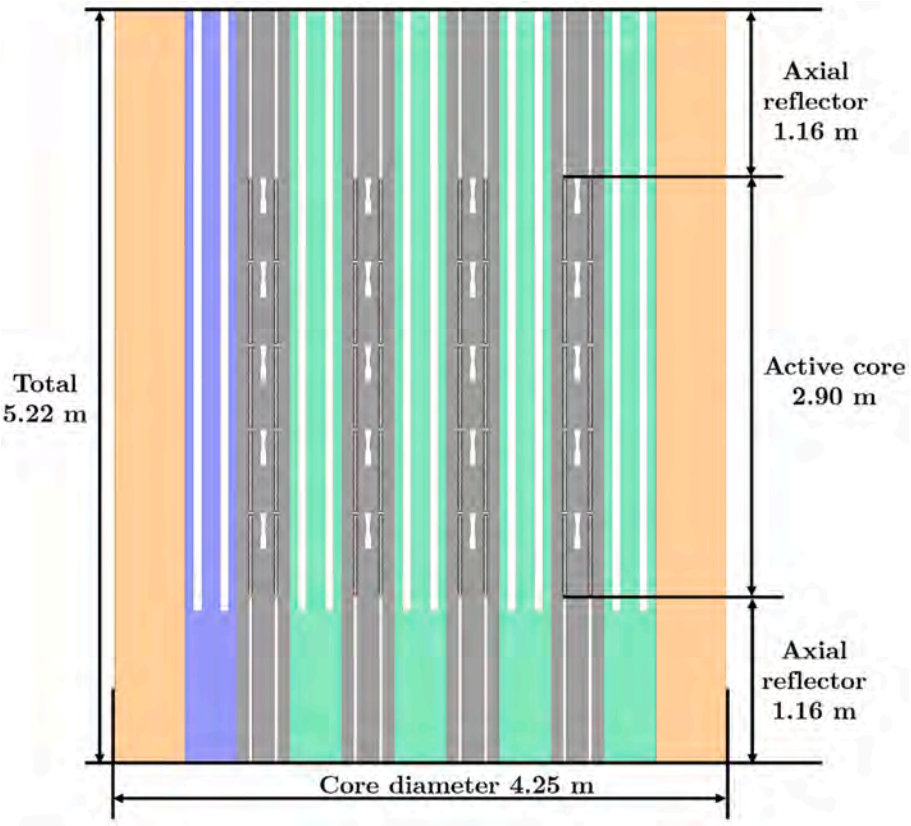


**Fig. 3.** The axial layout of HTTR.

maximum discharge burnup.

Afterward, the achievable core discharge burnup of the fuel block lattice having a different pair of design parameters (HM loading per fuel block and fissile content) is quantified using the non-linear reactivity method (Driscoll et al., 1991). In this method, the reactivity of the fuel block lattice is fitted into a polynomial equation as a function of the burnup cycle ($B_c$). Similar to the previous study (Hartanto and Liem, 2020), a quartic equation is used, as shown by Eq. (1). Before calculating the achievable discharge burnup ($B_d$), the burnup cycle ($B_c$) should be determined by taking into account the reactivity loss due to leakage in the core ($\rho_{leakage}$) and the number of the refueling batches ($N$), as shown by Eq. (2). It is worth mentioning that $\rho_{leakage}$ can be adjusted until the targeted discharge burnup is achieved in the core calculation. Lastly, the discharge burnup ($B_d$) is computed by using Eq. (3). The optimal fuel composition, which has the minimum fissile mass (kg) per unit energy generated (GWd), is then determined by taking into consideration the

**Table 2**
Block-type fuel lattice design parameters (Bess and Fujimoto, 2011).

| Coated fuel particle | (HTTR) |
|---|---|
| Fuel | (U-235/U-238)$O_2$ |
| Fuel density (g/cm$^3$) | 10.40363 |
| Uranium enrichment (w/o) | <20% |
| Burnable poison material | Natural Boron |
| Type | TRISO |
| Kernel diameter (mm) | 0.600 |
| Particle diameter (mm) | 0.920 |
| Coating material | PyC/PyC/SiC/PyC |
| Thickness (mm) | 0.060/0.030/0.025/0.045 |
| Density (g/cm$^3$) | 1.100/1.850/3.200/1.850 |
| Packing fraction (v/o) | Variable < 30% |
| Fuel compact | (HTTR) |
| Inner diameter (cm) | 1.00 |
| Outer diameter (cm) | 2.60 |
| Matrix density (g/cm$^3$) | 1.70 |
| Graphite sleeve | |
| Inner diameter (cm) | 2.60 |
| Outer diameter (cm) | 3.40 |
| Density (g/cm$^3$) | 1.77 |
| Coolant annulus channel | |
| Inner diameter (cm) | 3.40 |
| Outer diameter (cm) | 4.10 |
| Fuel block | |
| Flat to flat distance (cm) | 5.15 |
| No. of fuel pin | 31 or 33 |
| No. of BP holes | 3 |
| BP channel diameter (cm) | 1.5 |
| No. of central handling socket | 1 |
| Handling socket depth (cm) | 25.0 |
| Top and bottom graphite layer thickness (cm) | 1.7 |
| Matrix density (g/cm$^3$) | 1.7512 |

discharge burnup.

$$\rho(B_c) = a_0 + a_1 B_c + a_2 B_c^2 + a_3 B_c^3 + a_4 B_c^4 \quad (1)$$

$$\frac{1}{N}\sum_{i=1}^{N} \rho(iB_c) = \rho_{leakage} \quad (2)$$

$$B_d = NB_c \quad (3)$$

In the second step, the full core burnup calculation is performed. The fissile content and HM loading per fuel block of the optimal fuel composition from the first step cannot be used directly in this step. Typically, an HTGR core consists of not only fuel block but a considerable amount of graphite blocks which will alter $N_C/N_{HM}$ of the core. Also, an HTGR is surrounded by a thick layer of radial and axial graphite reflectors and it also increases the $N_C/N_{HM}$ of the core significantly compared to that of the fuel block lattice. An equivalent $N_C/N_{HM}$between lattice and core can be obtained by increasing the TRISO particle fuel packing fraction in the core so that the optimal fuel composition from the lattice calculations can be adopted, i.e. projected into the core, as illustrated in Fig. 1. One should be cautious that the "importance" of graphite in the graphite blocks and of the graphite reflectors is different compared to the "importance" of graphite in the fuel blocks. Hence, a simple volume-weighted $N_C/N_{HM}$ relationship would not project the optimal lattice $N_C/N_{HM}$ into the optimal core $N_C/N_{HM}$. In our previous study with a heuristic approach (Hartanto and Liem, 2020), the graphite blocks in the core are considered using a simple volume-weighted, while the graphite in the reflector region was not included in the $N_C/N_{HM}$.

A better approach is suggested in this paper by introducing the use of neutron importance $I(r)$, a well-known concept in the reactor physics field. One can easily understand intuitively that the effect or contribution of a graphite reflector located far away from the core to the $N_C/N_{HM}$ must be lower than a graphite block located inside the core. The neutron importance provides a quantitative as well as a systematic way to "weigh" the graphite contribution to the core equivalent $N_C/N_{HM}$. In the

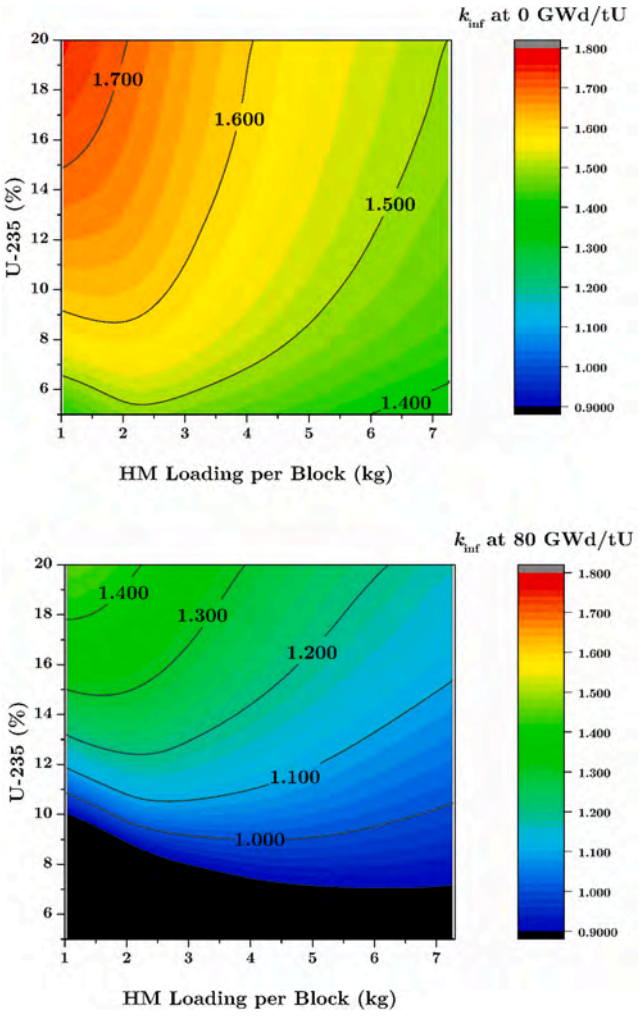


**Fig. 4.** Infinite neutron multiplication factor at 0 and 80 GWd/tU.

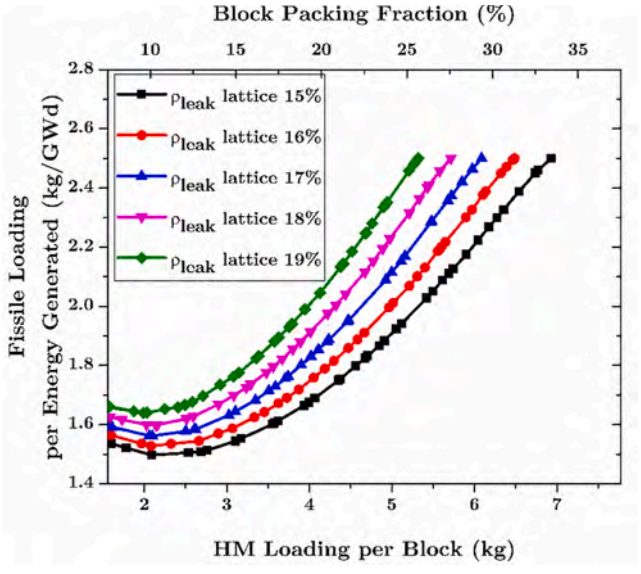


**Fig. 5.** Fissile loading per energy generated against HM loading per fuel block for single batch refueling scheme.

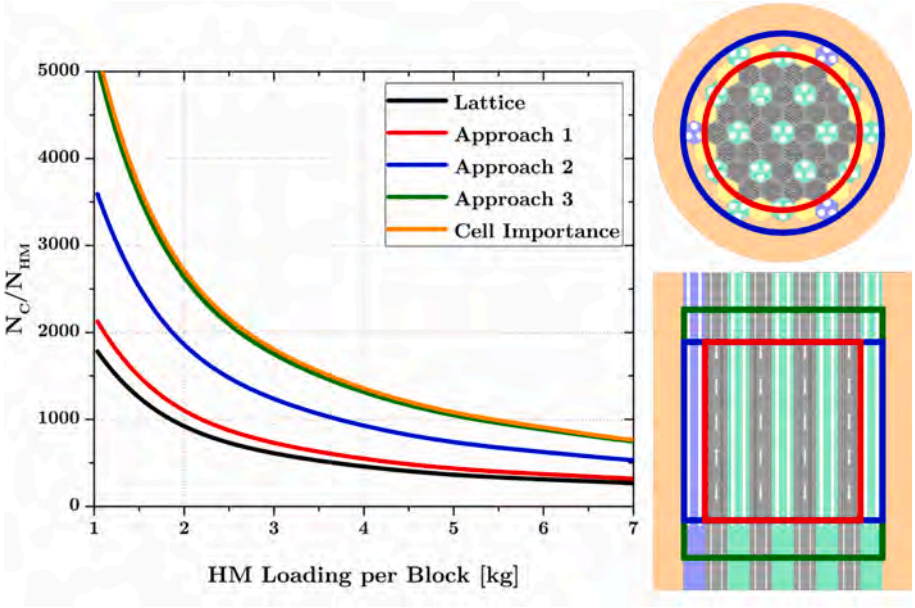


**Fig. 6.** $N_C/N_{HM}$ of lattice and core.

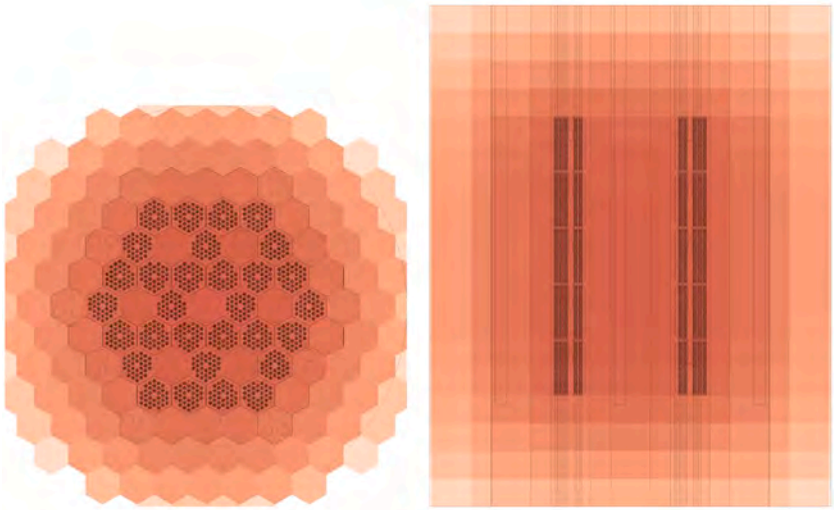

**Fig. 7.** Neutron importance distribution at the center of the core.

following, we will describe the new technique by using the Serpent 2 code but the technique is not limited by the analytical tool used. Even one can prepare the neutron importance by a deterministic code.

Serpent 2 has the capability to generate the neutron importance of the cell for the weight-window-based variance reduction based on the response matrix method (Leppänen, 2019). Two importance values are generated: 1) cellwise source important, defined as "a contribution of a single source particle emitted in energy group $g$ to the given global response", and 2) current importance, defined as "the response contribution of a particle entering the cell through the boundary in energy group $g$" (Leppänen, 2019). The neutron importance used in this study is the current importance in one group energy structure and the response is determined as the contribution of each mesh to the fission reaction. The mesh is defined as a hexagonal mesh with the same pitch as a fuel block and the height is half of the fuel block.

An eigenvalue mode calculation is first performed to collect and save the fission source distribution into a file to be used in the next step (neutron importance calculation). A fixed source mode calculation is then carried out to generate neutron importance using the previously saved fission source distribution. Several iterations are typically required until the result is converged. In this study, the total number of iterations is eight where the first three iterations are for the global variance reduction. Later, the $N_C$ of the core can be calculated by directly multiplying the normalized neutron importance of each mesh by the number of graphite atoms in each mesh, as shown in Eqs. (4) and (5).

$$\widetilde{N}_C = \frac{1}{V}\int_{Reactor} N_C(r)I(r)dr \tag{4}$$

$$\int I(r)dV = 1.0 \tag{5}$$

## 3. Application to small-sized HTGR design

The proposed technique is implemented in the Japanese High-Temperature Engineering Test Reactor (HTTR) (Bess and Fujimoto, 2011) to find the optimal fuel composition that can achieve an average core discharge burnup of 80 GWd/tU. HTTR is a block-type high

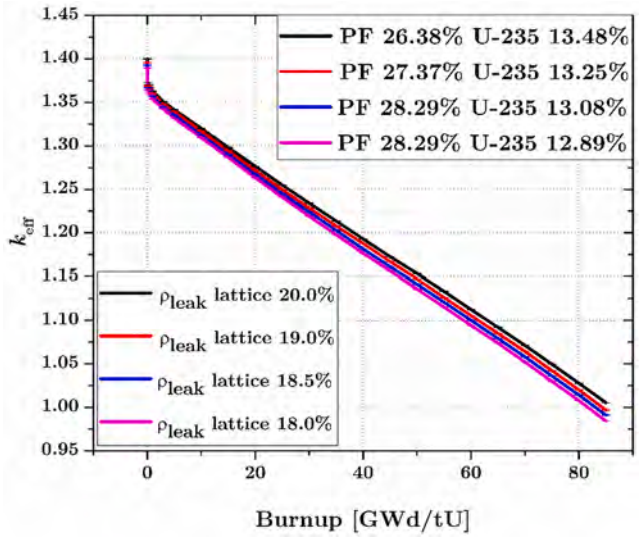


**Fig. 8.** $k_{\text{eff}}$ of the single-batch core using different values of lattice leakage reactivity.

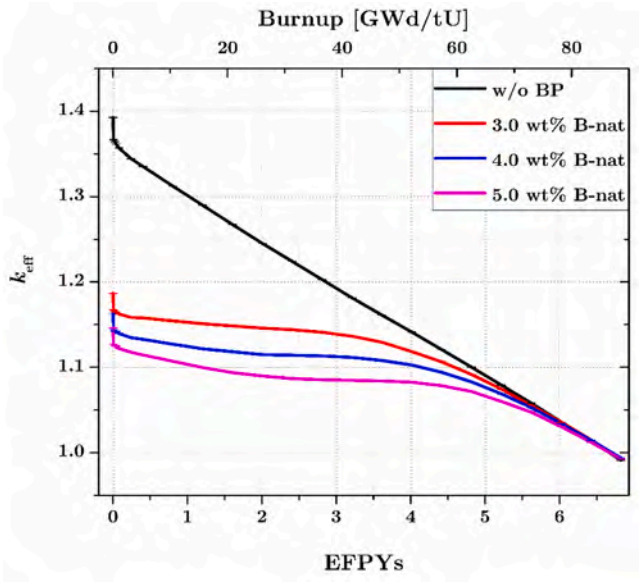


**Fig. 9.** $k_{\text{eff}}$ of single-batch core with burnable poison.

temperature helium-cooled graphite-moderated experimental reactor, produces 30 MWth power, and it is operated by Japan Atomic Energy Agency. The average and maximum core discharge burnup of HTTR is about 22 and 33 GWd/tU, respectively (JAERI, 1994).

The main design parameters of HTTR are summarized in Table 1. The core consists of 61 hexagonal columns surrounded by a thick permanent graphite reflector, as shown in Fig. 2. The columns are distributed such as 30 columns are for fuel, 16 columns for control rod, 3 columns for instrumentation, and the remaining 12 columns are for the replaceable reflector. The core has a diameter of 425 cm and a height of 522 cm. Each fuel column has five fuel blocks and two axial reflector blocks at the top and bottom, as illustrated in Fig. 3. In each control rod column as well as in the instrumentation column, three insertion holes with a diameter of 12.3 cm and a depth of 416 cm are located. The replaceable reflector column and the permanent reflector are made of graphite.

The fuel block lattice design parameters are tabulated in Table 2. The HTTR design uses two types of fuel block which are with 31 and 33 fuel pins. The fuel pin consists of an annular fuel compact enclosed in a

**Table 3**
Single batch core parameters.

| | |
|---|---|
| Fissile loading per energy generated (kg/GWd) | 1.635 |
| HM loading per block (kg) | 5.865 |
| Total HM mass in core (kg) | 879.773 |
| Fissile enrichment (wt%) | 13.08 |
| Fissile mass per block (kg) | 0.767 |
| Total fissile mass in core | 115.050 |
| TRISO fuel packing fraction | 28.29 |
| $N_C/N_{HM}$of fuel block | 323.917 |
| BP content | 4.0 wt% nat. B |
| Cycle length (years) | 6.42 |
| $k_{\text{eff}}$ | |
| BOC | 1.16300 ± 7 pcm |
| EOC | 1.01432 ± 6 pcm |
| FTC (pcm/K) | |
| BOC | −2.848 ± 0.072 |
| EOC | −3.551 ± 0.086 |
| MTC (pcm/K) | |
| BOC | −2.180 ± 0.023 |
| EOC | −3.275 ± 0.029 |
| Radial peak power BOC/EOC | 1.170/1.082 |
| Axial peak power BOC/EOC | 1.205/1.139 |

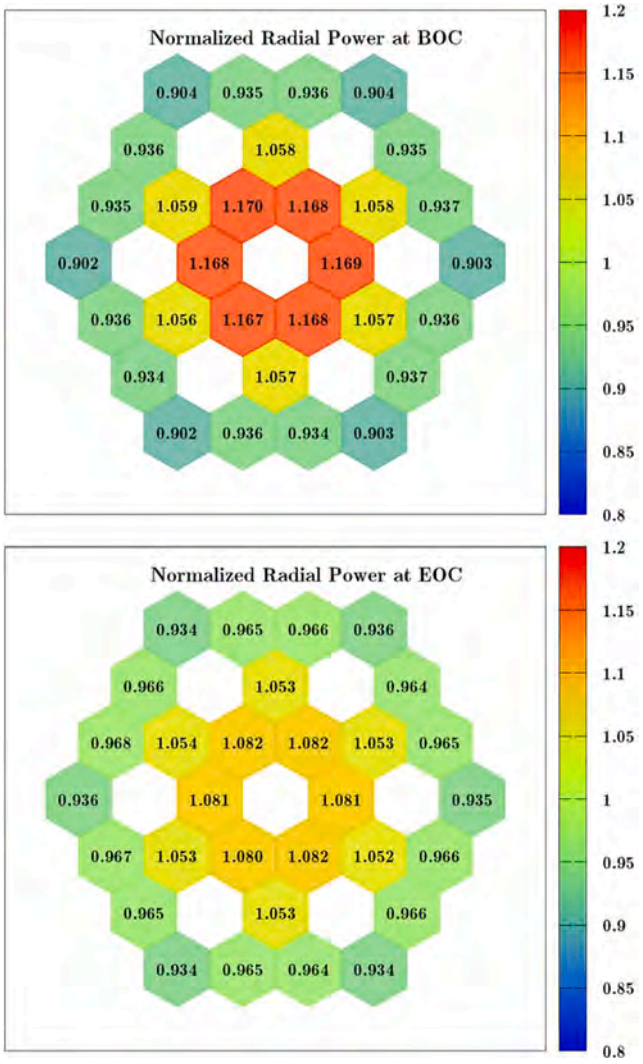


**Fig. 10.** Normalized radial power distribution of single-batch core with burnable poison.

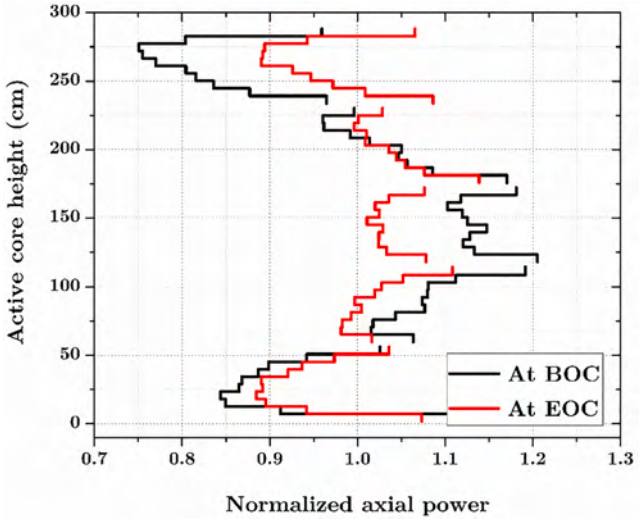


**Fig. 11.** The normalized axial power distribution of single-batch core with burnable poison.

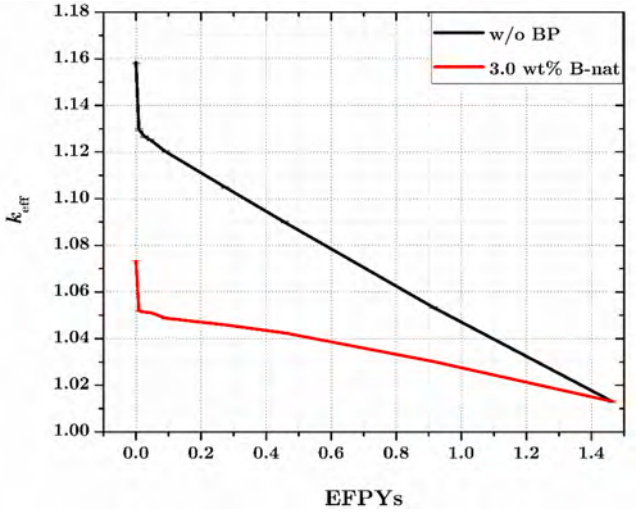


**Fig. 13.** $k_{eff}$ of a single-batch core with burnable poison.

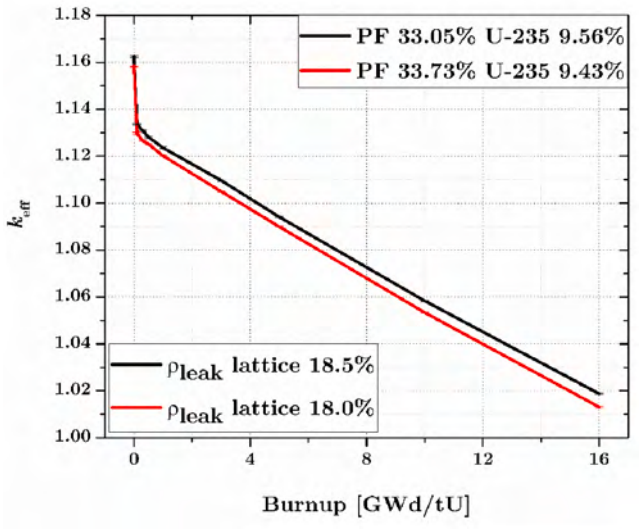


**Fig. 12.** $k_{eff}$ of the 5-batch core using different values of lattice leakage reactivity.

graphite sleeve. The fuel compact has an inner and outer radius of 0.5 cm and 1.3 cm, respectively, and it contains TRISO fuel particles with a radius of 0.046 cm dispersed in the graphite matrix. Low enriched uranium fuel is used in the TRISO fuel particle. In the HTTR, twelve different enrichments (from 3% to 10% U-235) are adopted depending on the fuel block location, for example, a lower enrichment is located near the center of the core. The fuel block of HTTR also has three burnable poison (BP) insertion holes with a radius of 0.75 cm. Another feature of the HTTR fuel block is the fuel handling socket located at its center. For the sake of simplicity, a fuel block with 33 fuel pins and a uniform enrichment is considered in this study.

### 3.1. Lattice physics optimization

The depletion calculation of the fuel block lattice was accomplished using Serpent 2. A 3-D model was considered, and a periodic boundary condition was applied in any direction. The TRISO fuel particles were treated explicitly and their positions were generated randomly. The calculation was performed with 15,000 neutron histories and 200 total

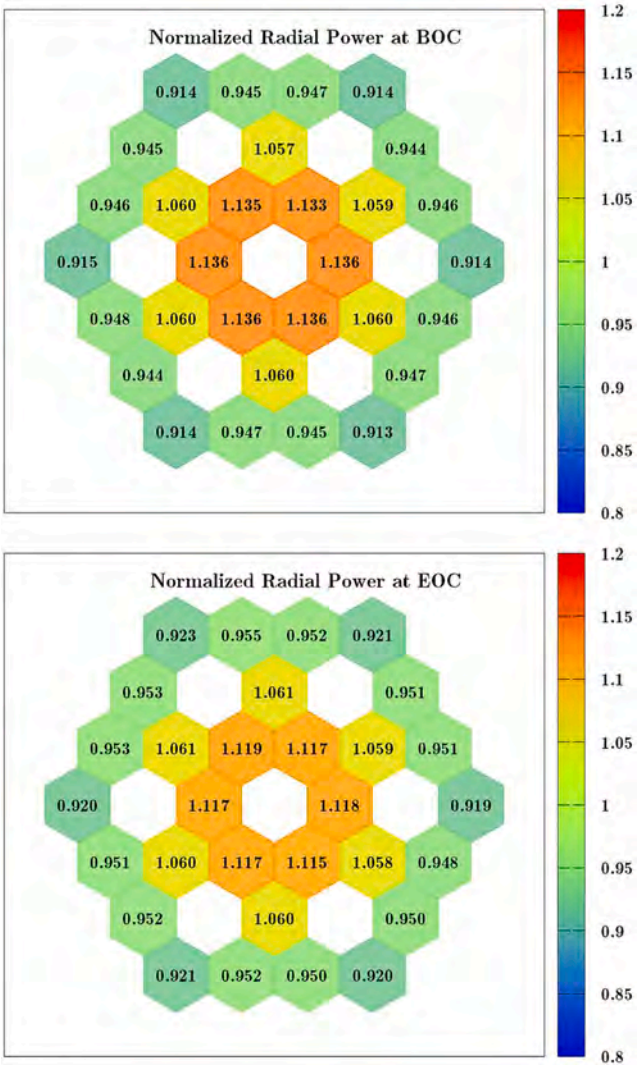


**Fig. 14.** The normalized radial power distribution of 5-batch core with burnable poison.

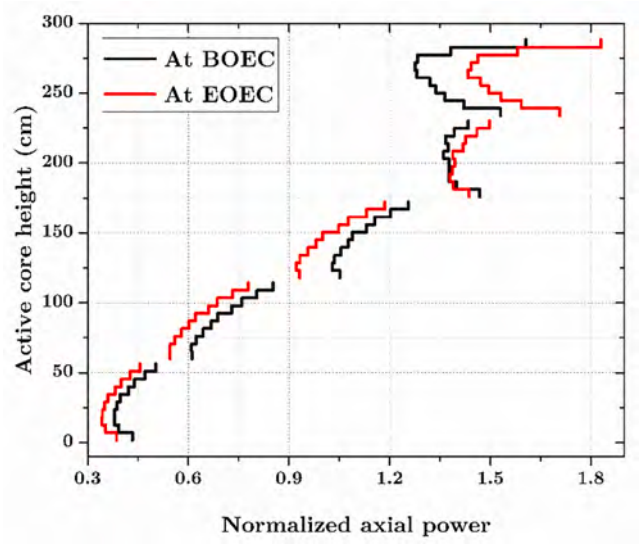


**Fig. 15.** The normalized axial power distribution of 5-batch core with burnable poison.

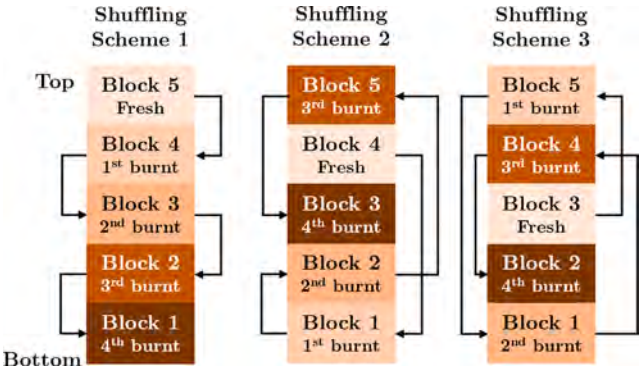


**Fig. 16.** Fuel block shuffling schemes.

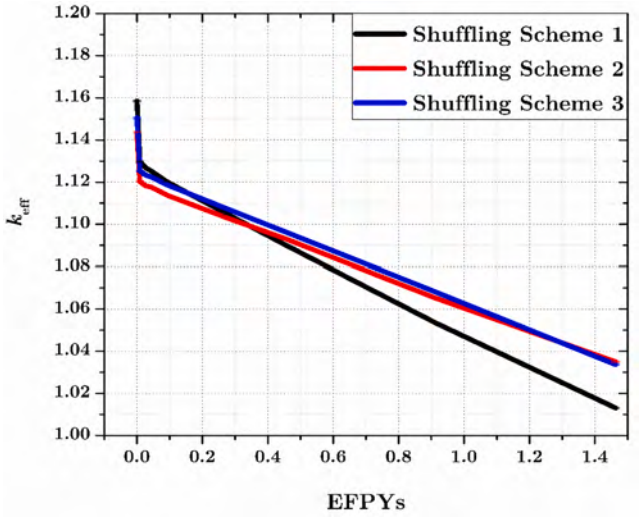


**Fig. 17.** $k_{eff}$ of 5-batch core using different shuffling schemes.

cycles, resulting in a statistical uncertainty of the neutron multiplication factor about 35–40 pcm. The latest nuclear data library ENDF/B-VIII.0 was used. Moreover, the thermal scattering law $S(\alpha,\beta)$ for graphite with 10% porosity was applied in the calculation as well as the Doppler broadening rejection correction (DBRC) option. The temperature used in the calculation was 1230 K for fuel compact and 1060 K for the graphite sleeve, graphite matrix, and helium coolant.

Fig. 4 shows the infinite multiplication factor $k_{inf}$ as functions of fuel enrichment and HM loading per fuel block, at the BOC (beginning of cycle or 0 GWd/tU) and EOC (end of cycle or 80 GWd/tU). A lower HM loading fuel block has a softer spectrum and it has a higher value of $k_{inf}$ compared to the higher HM loading fuel block with the same fuel enrichment. Additionally, certain fuel enrichment is also required to achieve the desired discharge burnup value.

Using the non-linear reactivity method, the fissile loading per energy generated is determined for several $\rho_{leakage}$ values and a quartic function is again used to fit the points, as depicted in Fig. 5. The optimum fuel composition is quantified by finding the root that gives the derivative of the fitting function equals zero. Later, this optimum fuel composition is used in the core using the projection technique discussed previously.

### 3.2. Single batch core optimization design

The first step to use the optimum fuel composition obtained from the fuel block lattice calculations is to calculate the $N_C/N_{HM}$ of the core, and later the $N_C/N_{HM}$ of the optimum fuel from lattice is projected to the core's so they become equal. Therefore, the TRISO fuel packing fraction in the core increases, but the fissile loading per energy generated and the fissile enrichment is still the same between lattice and core. The amount of graphite in the core should be reasonably considered. In Fig. 6, several approaches including the newly proposed technique are considered.

Approach 1 takes into account the graphite located in the center ring and the 3 rings of the fuel block, but the graphite in the axial reflectors is not considered, similar to the previous study (Hartanto and Liem, 2020). In approach 2, the graphite located in all hexagonal blocks is considered, but it also does not include the graphite in the axial reflectors. Approach 3 is similar to approach 2 but includes one block of the axial reflector at each top and bottom. The final approach is the use of neutron importance generated by Serpent 2 as plotted in Fig. 7 for the radial and axial directions. It is clear that the meshes near the center of the core have higher importance (darker color), however, the contribution of graphite reflectors is also considered. Therefore, the neutron importance approach is expected to produce an equivalently optimal $N_C/N_{HM}$, while approaches 1 and 2 underestimate the $N_C/N_{HM}$ noticeably.

Using the newly proposed projection technique, based on the neutron importance, the TRISO fuel packing fraction of the core can be obtained for each lattice neutron leakage reactivity. A depletion calculation is then performed to determine the optimum core fuel composition that can achieve discharge burnup of 80 GWd/tU, and the excess reactivity at this burnup step (EOC) is still about 1000 pcm to take into account the addition of the experimental apparatus installed in the core. The total neutron histories in the depletion calculation are 7 million neutrons, and 2 million neutrons are discarded in the inactive cycle. Moreover, the fuel blocks are divided into 3 radial and 5 axial burnup regions. It is evident that the number of full core depletion calculations can be significantly reduced since one does not need to conduct an exhaustive parametric survey to obtain the optimal $N_C/N_{HM}$.

Fig. 8 shows the evolution of $k_{eff}$ and the core can achieve the objective by having a TRISO fuel packing fraction of 28.29% and the fissile enrichment is 13.08%. The selected core is loaded with BP rods in all fuel blocks, and in each fuel block, 3 BP rods are embedded. The BP rod is the same used in HTTR; its radius is 0.7 cm, it consists of a natural enriched $B_4C/C$ composite with a density of 1.8 g/cm$^3$ and a length of 20 cm at each end joined by a 10 cm graphite. As illustrated in Fig. 9, the insertion of BP rods reduces the excess reactivity at BOC significantly and the boron content of 4% is selected as the reference core for this single batch scheme.

Other neutronics parameters of this core such as fuel temperature

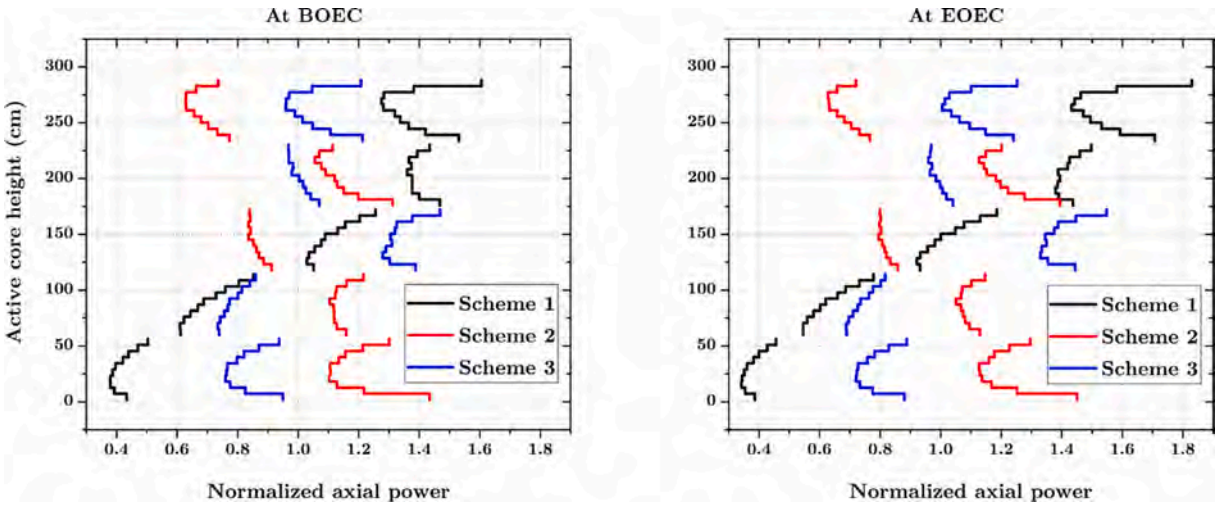


**Fig. 18.** Normalized axial power distribution of 5-batch core using different shuffling schemes.

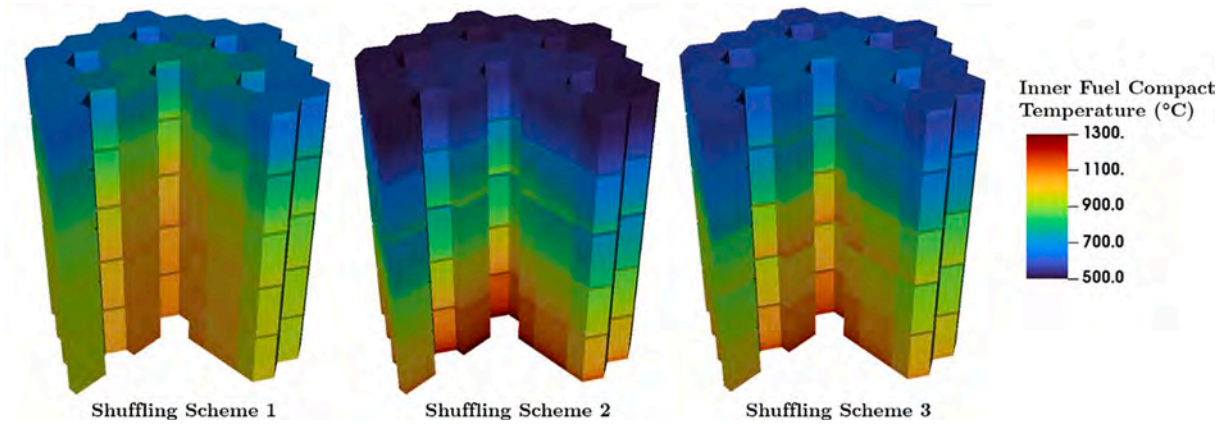


**Fig. 19.** Inner fuel compact temperature (°C) using different shuffling schemes.

reactivity coefficient (FTC) and moderator temperature reactivity coefficient (MTC) are presented in Table 3. The FTC is calculated by increasing the fuel compact temperature by 100 K, while the MTC is calculated by increasing the graphite sleeve and graphite matrix by 300 K. Both FTC and MTC values are negative at BOC and EOC. The normalized radial and axial power profiles are also presented in Figs. 10 and 11. The power profiles become slightly flat at EOC.

### 3.3. 5-Batch core optimization design

To increase the fuel utilization and minimize fuel enrichment, a multi-batch core is proposed, and in this case, it is a 5-batch refueling scheme because each fuel column has 5 fuel blocks. During the refueling, the fuel blocks are moved only along the axial direction, similar to those applied in VHTR (Kim et al., 2007). For our first try, the new fuel blocks are inserted from the top of the core and the discharged fuel blocks are taken out from the bottom of the core. The radial fuel shuffling is not considered. It is assumed that the refueling interval takes 30 days. The same calculation conditions and procedures are applied to get the optimum fuel composition for the 5-batch core.

Fig. 12 shows the $k_{eff}$ of the equilibrium cycle and it is observed that the target discharge burnup is satisfactorily achieved by having a TRISO fuel packing fraction of 33.73% and fissile enrichment of 9.43%. As expected, a multi-batch core requires much lower enrichment compared to a single batch core, however, the total HM mass is higher for a multi-batch core. The selected core is then loaded with BP rods in the same way as in the previous section. It is shown in Fig. 13 that the excess reactivity can be suppressed significantly with 3 wt% boron in the BP rods. Other results worth discussing are the radial and axial power profiles at the beginning of the equilibrium cycle (BOEC) and end of the equilibrium cycle (EOEC) as depicted in Figs. 14 and 15. The radial power profile has a similar trend to the single batch core, however, the axial power profile has a peak value of 1.830 located in the fresh fuel region near the boundary of graphite axial reflector at EOEC. The HTTR design has a peak value of 1.7 for axial power. To reduce this value, different shuffling schemes are proposed.

Two other fuel shuffling schemes are suggested, as illustrated in Fig. 16. Shuffling scheme 1 is initially applied. In shuffling schemes 2 and 3, the fresh fuel block is moved to the center and it is surrounded by the burned fuel blocks. This approach is expected to reduce the axial power peak in the fresh fuel region. The $k_{eff}$ at the equilibrium cycle for the 3 shuffling schemes are compared in Fig. 17 and they achieve the target discharge burnup. It is also noticed that the excess reactivity slightly reduces in the new shuffling schemes. However, as shown in Fig. 18, the new shuffling schemes significantly decrease the peak axial power, from 1.83 to 1.55.

To complete the study, the temperature analysis is also performed to investigate the impact of fuel shuffling on the fuel temperature. The temperature calculation is carried out along the fuel columns. The helium coolant with a pressure of 4 MPa enters the core at a temperature of 350 °C and exits at a temperature of 950 °C. Serpent 2 provides the power density, and for this purpose, the power density is tallied for each

**Table 4**
5-batch core parameters.

| | |
|---|---|
| Fissile loading per energy generated (kg/GWd) | 1.178 |
| HM loading per block (kg) | 6.993 |
| Total HM mass in core (kg) | 1048.945 |
| Fissile enrichment (wt%) | 9.43 |
| Fissile mass per block (kg) | 0.659 |
| Total fissile mass in core | 98.874 |
| TRISO fuel packing fraction | 33.73 |
| $N_C/N_{HM}$ of fuel block | 323.074 |
| BP content | 3.0 wt% nat. B |
| Cycle length (years) | 1.53 |
| $k_{eff}$ at BOEC/EOEC | |
| Shuffling scheme 1 | 1.07349 ± 7 pcm/1.01330 ± 6 pcm |
| Shuffling scheme 2 | 1.07087 ± 7 pcm/1.01065 ± 6 pcm |
| Shuffling scheme 3 | 1.07145 ± 7 pcm/1.01205 ± 6 pcm |
| FTC (pcm/K) at BOEC/EOEC | |
| Shuffling scheme 1 | −3.633 ± 0.083/−3.528 ± 0.091 |
| Shuffling scheme 2 | −3.519 ± 0.087/−3.636 ± 0.092 |
| Shuffling scheme 3 | −3.778 ± 0.081/−3.636 ± 0.090 |
| MTC (pcm/K) at BOEC/EOEC | |
| Shuffling scheme 1 | −2.746 ± 0.027/−2.325 ± 0.031 |
| Shuffling scheme 2 | −2.801 ± 0.029/−2.443 ± 0.031 |
| Shuffling scheme 3 | −2.996 ± 0.028/−2.899 ± 0.031 |
| Radial peak power at BOEC/EOEC | |
| Shuffling scheme 1 | 1.136/1.119 |
| Shuffling scheme 2 | 1.135/1.118 |
| Shuffling scheme 3 | 1.135/1.119 |
| Axial peak power at BOEC/EOEC | |
| Shuffling scheme 1 | 1.606/1.830 |
| Shuffling scheme 2 | 1.434/1.451 |
| Shuffling scheme 3 | 1.468/1.548 |
| Max. inner compact fuel temp (°C) | |
| Shuffling scheme 1 | 1099.87 |
| Shuffling scheme 2 | 1295.15 |
| Shuffling scheme 3 | 1195.57 |

fuel column and each column is divided into 50 axial zones. The equations used in the calculations are taken from Maruyama et al. (1994) and Inaba and Nishihara (2017). The inner fuel compact temperature is sketched in Fig. 19, and the maximum fuel temperature is 1099.87 °C, 1295.15 °C, 1195.57 °C for shuffling schemes 1, 2, and 3, respectively. Although the peak axial power is relatively high in shuffling scheme 1, the maximum fuel temperature is slightly lower than in the other shuffling schemes because the cold helium coolant flows into the core from the top where the peak axial power occurs. In shuffling scheme 2, the maximum fuel temperature can reach up to 1295.15 °C since the peak axial power occurs at the bottom of the core near the exit coolant path. Meanwhile, the maximum fuel temperate in shuffling scheme 3 is about 100 °C lower than shuffling scheme 2. Table 4 summarizes and compares the performance of the 5-batch cores. The FTC and MTC are also presented and they are always negative during the operation.

## 4. Conclusion and future work

A new technique based on the neutron importance concept to make a projection of the optimal design parameters obtained from the fuel design phase to the full core design phase of HTGR has been proposed and applied to the HTTR operating in a single-batch and 5-batch refueling schemes. In the first step, the fuel composition of the fuel lattice is optimized to have a minimum fissile content per energy generated (kg/GWd). In the second step, the core calculation is performed. The $N_C/N_{HM}$ of the core is calculated by considering the neutron importance of each region to the fission reaction and later the $N_C/N_{HM}$ of the optimum fuel from lattice is projected to the core's, so they are equal. The TRISO fuel packing fraction in the core increases, but the fissile loading per energy generated and the fissile enrichment is still the same between lattice and core.

The design objective of this study which is to achieve an average core discharge burnup of 80 GWd/tU can be achieved by both single-batch and 5-batch refueling schemes. The FTC and MTC are also always negative. However, 5-batch refueling scheme gives more advantages such as lower fissile enrichment, lower fissile loading per energy generated, and slightly longer fuel residence time.

## CRediT authorship contribution statement

**Donny Hartanto:** Conceptualization, Methodology, Software, Formal analysis, Validation, Investigation, Data curation, Writing - original draft, Writing - review & editing, Visualization. **Peng Hong Liem:** Conceptualization, Methodology, Validation, Writing - original draft, Writing - review & editing, Supervision.

## Declaration of Competing Interest

The authors declare that they have no known competing financial interests or personal relationships that could have appeared to influence the work reported in this paper.

## Acknowledgments

The authors would like to thank Dr. Min-Jae Lee of the Korea Atomic Energy Research Institute (KAERI) for his assistance in using VisIt visualization software. D. Hartanto also acknowledge the use of the HPC Facility at the University of Sharjah for part of the work reported in this paper.

## References

Bahadir, T., Lindahl S.O. (2009). Studsvik's Next Generation Nodal Code Simulate-5, Proceedings of Advances in Nuclear Fuel Management IV (ANFM 2009), Hilton Head Island, South Carolina, USA, April 12-15.

Bess J.D., Fujimoto N. (2011). Evaluation of the Start-up Core Physics Tests at Japan's High Temperature Engineering Test Reactor (Fully-loaded Core), HTTR-GCRRESR-001, Rev. 1, in International Handbook of Evaluated Reactor Physics Benchmark Experiments, NEA/NSC/DOC(2006)1, Organisation for Economic Co-operation and Development/Nuclear Energy Agency.

Brown D.A. et al. (2018). ENDF/B-VIII.0: The 8th Major Release of the Nuclear Reaction Data Library with CIELO-project Cross Sections, New Standards and Thermal Scattering Data, Nuclear Data Sheets 148, 1-42.

Driscoll, M.J., et al., 1991. The Linear Reactivity Model for Nuclear Fuel Management. American Nuclear Society, La Grange Park, IL.

JAERI, 1994. Design of High Temperature Engineering Test Reactor (HTTR), JAERI-1332. Japan Atomic Energy Research Institute.

Hartanto, D., Liem, P.H., 2020. Physics Study of Block/Prismatic-Type HTGR Design Option for the Indonesian Experimental Power Reactor (RDE). Nucl. Eng. Design 368, 110821.

Inaba, Y., Nishihara, T., 2017. Development of fuel temperature calculation code for HTGRs. Ann. Nucl. Energy 101, 383–389.

Kim, Y., Jo, C.K., Noh, N.J., 2007. Axial block shuffling in a block-type VHTR for improved core performances. Transactions of the Korean Nuclear Society Autumn Meeting, Pyeong Chang, Korea, October 25-26.

Leppänen, J., et al., 2015. The Serpent Monte Carlo code: status, development and applications in 2013. Ann. Nucl. Energy 82, 142–150.

Leppänen, J., 2019. Response matrix method-based importance solver and variance reduction scheme in the serpent 2 Monte Carlo Code. Nucl. Technol. 205, 1416–1432.

Maruyama, S., et al., 1994. Evaluation of core thermal and hydraulic characteristics of HTTR. Nucl. Eng. Design 152, 183–196.

Nagaya, Y., Okumura, K., Sakurai, T., Mori, T. (2017). MVP/GMVP Version 3: General Purpose Monte Carlo Codes for Neutron and Photon Transport Calculations Based on Continuous Energy and Multigroup Methods. JAEA-Data/Code 2016-018, Japan Atomic Energy Agency.

Price, M.S.T., 2012. The dragon project origins, achievements and legacies. Nucl. Eng. Design 251, 60–68.

Rhodes, J., Smith, K., Lee, D. (2006). CASMO-5 Development and Applications, Proceedings of PHYSOR-2006, Vancouver, BC, Canada, September 10-14.

Werner, C.J. (ed.) (2017). MCNP User's Manual – Code Version 6.2, LA-UR-17-29981, Los Alamos National Laboratory.